Characterization of large rearrangements in autosomal dominant polycystic kidney disease and the PKD1/TSC2 contiguous gene syndrome

Article *in* Kidney International · October 2008

DOI: 10.1038/ki.2008.485 · Source: PubMed

CITATIONS
84

READS
152

21 authors, including:

Mark B Consugar
Massachusetts Eye and Ear Infirmary
43 PUBLICATIONS **2,364** CITATIONS
SEE PROFILE

Wai Chong (Vivian) Wong
Beth Israel Deaconess Medical Center
163 PUBLICATIONS **976** CITATIONS
SEE PROFILE

Denise L Walker
Mayo Foundation for Medical Education and Research
29 PUBLICATIONS **1,621** CITATIONS
SEE PROFILE

Characterization of large rearrangements in autosomal dominant polycystic kidney disease and the PKD1/TSC2 contiguous gene syndrome

Mark B. Consugar[1], Wai C. Wong[1], Patrick A. Lundquist[2], Sandro Rossetti[1], Vickie J. Kubly[1], Denise L. Walker[1], Laureano J. Rangel[3], Richard Aspinwall[4], W. Patrick Niaudet[5], Seza Özen[6], Albert David[7], Milen Velinov[8], Eric J. Bergstralh[3], Kyongtae T. Bae[9], Arlene B. Chapman[10], Lisa M. Guay-Woodford[11], Jared J. Grantham[12], Vicente E. Torres[1], Julian R. Sampson[13], Brian D. Dawson[2] and Peter C. Harris[1] for the CRISP Consortium

[1]Division of Nephrology and Hypertension, Department of Medicine, Mayo Clinic, Rochester, Minnesota, USA; [2]Department of Laboratory Medicine and Pathology, Mayo Clinic, Rochester, Minnesota, USA; [3]Division of Biostatistics, Department of Health Sciences Research, Mayo Clinic, Rochester, Minnesota, USA; [4]Weatherall Institute of Molecular Medicine, University of Oxford, Headington, Oxford, UK; [5]Service de Néphrologie Pédiatrique, Hôpital Necker-Enfants Malades, Paris, France; [6]Department of Pediatrics, Hacettepe University Faculty of Medicine, Ankara, Turkey; [7]Service de Génétique Médicale, Centre Hospitalier Universitaire, Nantes, France; [8]Department of Human Genetics, NY State Institute for Basic Research in Developmental Disabilities, Staten Island, New York, USA; [9]Department of Radiology, University of Pittsburgh, Pittsburgh, Pennsylvania, USA; [10]Division of Nephrology, Department of Medicine, Emory University School of Medicine, Atlanta, Georgia, USA; [11]Division of Genetics and Translational Medicine, Department of Medicine, University of Alabama at Birmingham, Birmingham, Alabama, USA; [12]Kidney Institute and Department of Internal Medicine, Kansas University Medical Center, Kansas City, Missouri, USA and [13]Institute of Medical Genetics, Cardiff University, Cardiff, Wales, UK

Large DNA rearrangements account for about 8% of disease mutations and are more common in duplicated genomic regions, where they are difficult to detect. Autosomal dominant polycystic kidney disease (ADPKD) is caused by mutations in either *PKD1* or *PKD2*. *PKD1* is located in an intrachromosomally duplicated region. A tuberous sclerosis gene, *TSC2*, lies immediately adjacent to *PKD1* and large deletions can result in the *PKD1/TSC2* contiguous gene deletion syndrome. To rapidly identify large rearrangements, a multiplex ligation-dependent probe amplification assay was developed employing base-pair differences between *PKD1* and the six pseudogenes to generate *PKD1*-specific probes. All changes in a set of 25 previously defined deletions in *PKD1*, *PKD2* and *PKD1/TSC2* were detected by this assay and we also found 14 new mutations at these loci. About 4% of the ADPKD patients in the CRISP study were found to have gross rearrangements, and these accounted for about a third of base-pair mutation negative families. Sensitivity of the assay showed that about 40% of *PKD1/TSC* contiguous gene deletion syndrome families contained mosaic cases. Characterization of a family found to be mosaic for a *PKD1* deletion is discussed here to illustrate family risk and donor selection considerations. Our assay improves detection levels and the reliability of molecular testing of patients with ADPKD.

Kidney International advance online publication, 24 September 2008; doi:10.1038/ki.2008.485

KEYWORDS: ADPKD; *PKD1/TSC2*-CGS; MLPA; deletions; mosaic; *PKD2*

Correspondence: *Peter C. Harris, Division of Nephrology and Hypertension, Mayo Clinic, 200 First Street SW, Rochester, Minnesota 55905, USA. E-mail: harris.peter@mayo.edu*

Received 1 May 2008; revised 30 June 2008; accepted 8 July 2008

Autosomal dominant polycystic kidney disease (ADPKD) is a common cause of end-stage renal disease (ESRD) due to progressive cyst development and enlargement.[1] ADPKD is genetically heterogeneous with *PKD1* (46 exons; 16p13.3) accounting for ~85% of cases and *PKD2* (15 exons; 4q21) ~15%.[2–5] Immediately adjacent to *PKD1* lies *TSC2*, the most common gene for tuberous sclerosis (TSC), a dominantly inherited disorder characterized by the development of benign hamartomas in multiple organs and often resulting in mental retardation/behavioral problems.[6] The majority of *PKD1* (~40 kb, encoding exons 1–33) lies in a genomic region that is intrachromosomally, segmentally duplicated with six variously rearranged *PKD1*-like pseudogenes (*PKD1P1-P6*) located in 16p13.1.[2,7] As *PKD1P1-P6* have 99% sequence similarity to *PKD1*, protocols utilizing the rare mismatches with *PKD1* have been required to specifically amplify *PKD1* for mutation analysis.[8]

Base-pair screening strategies have identified mutations in ~87% of ADPKD patients, including the well-characterized Consortium for Radiological Imaging Studies of PKD (CRISP) population.[5] The majority of mutations are predicted to truncate the protein, but a quarter are missense.

Analysis by field inversion gel electrophoresis revealed that 2–3% of *PKD1* mutations are large deletions that remove one to multiple exons,[2,5,9] a lower level than the 8% estimated for mutations genome wide.[10] One *PKD2* deletion and several cases with additional phenotypes removing larger regions have been described.[11,12] Large *PKD1* deletions that also disrupt the adjacent *TSC2* gene result in a contiguous gene syndrome (CGS) with a distinctive phenotype of early onset PKD plus various manifestations of TSC.[13–20] Approximately 50 *PKD1/TSC2* deletion patients have been described with an average age of 20 years at ESRD.[18] However, some *PKD1/TSC2*-CGS patients have milder renal disease and one factor associated with a variable phenotype is mosaicism (only some cells harbor the deletion as the mutation occurred early in development), noted in 10 cases.[15,18]

The difficulty of screening for large rearrangements by gel and fluorescence *in situ* hybridization methods may underestimate the level of ADPKD deletion mutations. Multiplex ligation-dependent probe amplification (MLPA) is a recently developed, highly quantitative method that allows detection of deletions or duplications of exons and has been used to detect large rearrangements in a range of human diseases, including TSC.[15,21,22] MLPA utilizes two tagged primers that lie immediately adjacent in the genome that can only serve as a PCR template once they are ligated. This method has the advantage of speed and high-throughput compared to conventional deletion/duplication detection methods. We describe here an assay utilizing FlexMAP beads and the Luminex instrument to screen the ADPKD genes and *PKD1/TSC2*-CGS cases and characterize the large rearrangements detected.

RESULTS

Assay design

MLPA probes were designed to assay for gross deletions/duplications to *PKD1*, *PKD2*, and *PKD1/TSC2*, including flanking regions. Nine probes were located in the single copy exons of *PKD1* (exons 34–46); one in each of the *PKD2* exons, plus two flanking probes (total region ~120 kb); six in *TSC2*; and ten in genes flanking *PKD1/TSC2*, six up to 150 kb centromeric to *PKD1*, and four up to 80 kb telomeric to *TSC2* (total region 320 kb; see Figure 1 and Supplementary Table S1 for details). In the duplicated region of *PKD1* (exons 1–33), 12 exonic probes plus one to IVS2 were designed. To obtain locus specificity, the 3′ end of the short MLPA probe was positioned at a mismatch with all the *PKD1P1-P6* pseudogenes (see Supplementary Table S1). Two probes within the single copy area 1–1.5 kb 5′ to *PKD1* exon 1 were also developed. In all assays, four probes to autosomal genes elsewhere in the genome and an X-chromosomal marker, *DMD*, were employed as controls; males showed an ~50% decrease in signal associated with the presence of just one X chromosome (Figure 2).

Characterization of known deletions

To test the specificity of the probes, especially those in the duplicated part of *PKD1*, DNA from a total of 18 *PKD1/TSC2*-CGS families[18] were analyzed by MLPA (See Table 1 and Figure 1 for details). Cases 8, 11, 12, 14, and 16 are illustrated (Figure 2) and, as expected, all (except 16) showed deletion of both *PKD1* and *TSC2* with one (12) also deleted for *SLC9A3R2*, 5′ to *TSC2*. Several others (8, 11, and 14) removed one or more genes 5′ to *PKD1*. Previous analysis of case 16 showed that it removed just 84 bp at the 3′ end of the *TSC2*-coding region, but did not delete the exon 41 MLPA probe.[18] All 18 cases showed complete correspondence between the MLPA-defined-deleted region and the previous gel and fluorescence *in situ* hybridization-based analysis (except in sample 20; see below).

To further test the assay, six ADPKD cases with known intragenic *PKD1* deletions were analyzed. All deletions were confirmed with at least one MLPA probe showing the expected reduction in signal in the appropriate area (Figures 3 and 4 and Table 1). For *PKD2*, DNA from a patient with a large deletion of 4q21.1→21.3, including *PKD2*,[12] showed the expected signal reduction for all probes (Figure 5).

Previous studies showed that a significant proportion of *PKD1/TSC2*-CGS cases were somatic mosaics;[18] a particular challenge to detection by MLPA. Previously defined mosaic cases (19, 20, and 22) showed a reduction of copy number in the deleted area significantly less than the 50% associated with deletion in every cell (see Figure 6, 'Materials and Methods', and Table 1 for details). Interestingly, the deletion in case 20 was found to extend further centromeric than previously defined (Figures 1 and 6),[18] whereas two other previously described non-mosaic deletions (4 and 6) were found to be mosaics (Table 1). Two previously defined familial cases where a mosaic parent transmitted the deletion to their offspring were also analyzed. In family 7, the mosaic deletion in the mother (M7) was detected, but the low level of deleted cells in F13 was not clearly visible from the MLPA analysis.

A family with a *PKD1* mosaic mutation

Further analysis of the previously characterized 9.2 kb deletion in family 301157[5] confirmed the deletion in a sibling (R1502; Figure 3b), but surprisingly, the deletion was not detected in the father (F301157) by MLPA despite him having clear ADPKD with ESRD at 55 years. Amplification across the breakpoint identified a 1.7 kb deletion-specific fragment in the proband and at a much lower level in the father (Table 1). Southern analysis with a 3′ *PKD1* probe showed the breakpoint product present at a low level in the father. These results indicate that F301157 is a somatic mosaic with ~15% of cells harboring the deletion in leukocyte DNA. This is consistent with F301157 having a *de novo* change, with no known PKD in his parents or his seven siblings.

Novel ADPKD mutations

To determine the frequency of large DNA rearrangements in typical ADPKD, the CRISP cohort was analyzed. After sequence analysis, no mutations were defined in 26 families, whereas a further 53 had nondefinite mutations (mainly

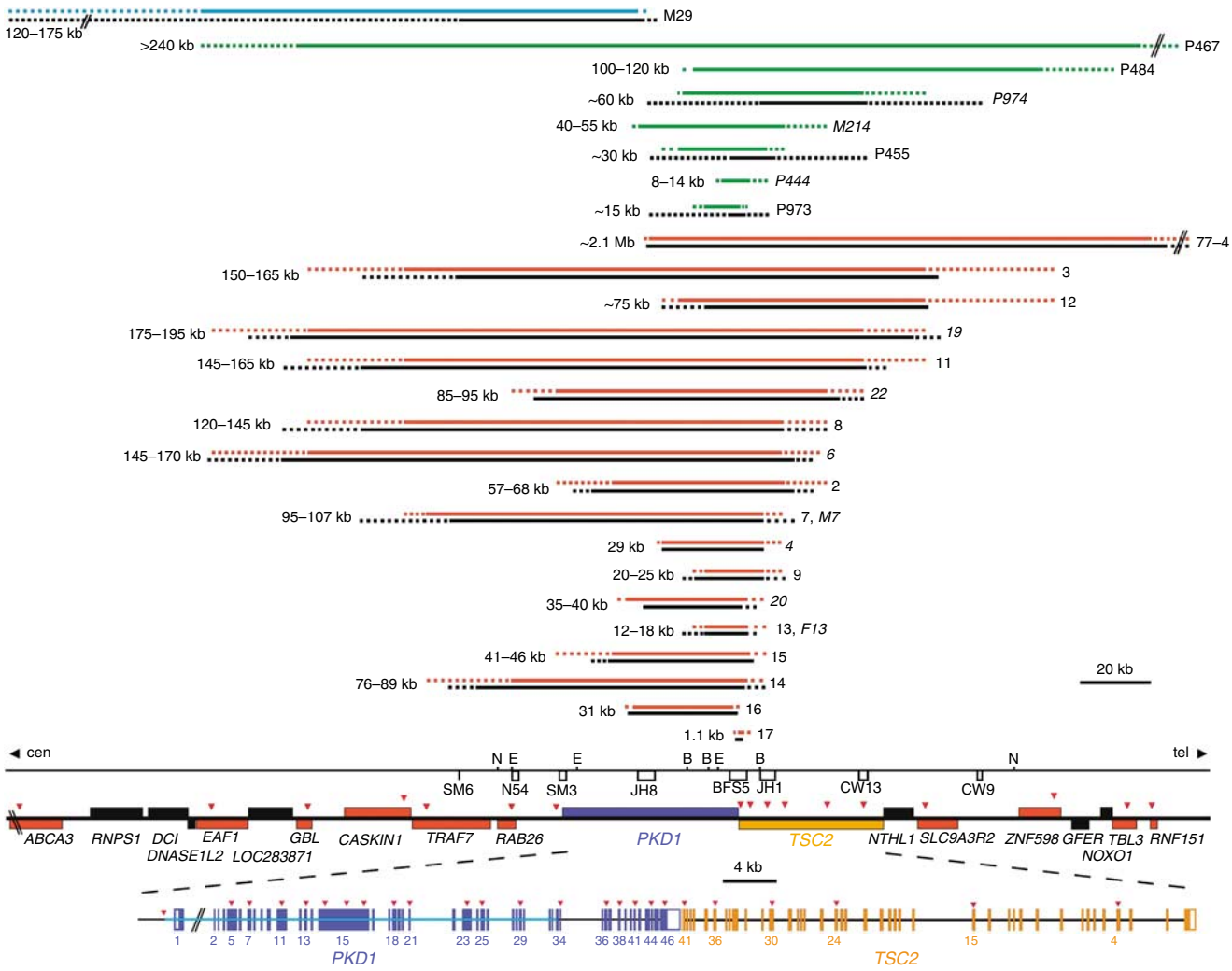

Figure 1 | Diagram showing the defined regions deleted in patients with the *PKD1/TSC2*-CGS. Upper part of the map shows: hybridization probes (open boxes); the SM6 microsatellite; relevant restriction sites for *Eco*RI (E), *Bam*HI (B) and *Nru*I (N); and centromeric (cen) and telomeric (tel) directions. Lower map shows the positions of *PKD1*, *TSC2*, and flanking genes in 16p13.3; transcribed telomeric above the line, and centromeric below; plus positions of MLPA probes (red arrowheads; tagged genes are in red). The intron/exon structures of *PKD1* and *TSC2* are shown at the bottom with positions of MLPA probes and the duplicated region of *PKD1* indicated with a light blue bar. The deleted region detected by MLPA for each subject is shown in red (or green for the newly described cases) and in black for previous gel-based analyses (Table 1). The family identifier and the best estimate of the size of the deleted region is indicated. Mosaic cases are italicized. The large deletion in M29 that just has an ADPKD phenotype is shown at the top (blue for the MLPA analysis).

missense).[5] All 79 cases were screened by MPLA and 4 new cases from the mutation negative group revealed large rearrangements (four large deletions had also previously been defined; Table 1 and Figures 3 and 4[5]). A 21 kb deletion detected in 493328 was fully characterized by amplification across the breakpoint and sequencing (Table 1 and Figures 3a and 4). A deletion of 48–87 kb in 407132 removed exons 1–21 of *PKD1*, plus the flanking gene, *RAB26*. In family 100009, two probes immediately 5′ to exon 1 were deleted in three affected family members (Figure 7a). To confirm that the mutation disrupted the gene, field inversion gel electrophoresis showed a ~2.5 kb deletion of an exon 1 containing genomic fragment (Figure 7a) that was not detected with an exon 1 probe (SM3). Case 259940 showed increased signal with the exon 18 MLPA probe and long range (LR)-PCR revealed a slightly larger product characterized as a 246 bp duplication of IVS17 and including 119 bp of exon 18 (Table 1 and Figure 7b). The total frequency of large rearrangements in the CRISP population was therefore 8 of 202 (4%).

Screening further base-pair mutation-negative ADPKD samples revealed three additional deletions. In M143, a 1.5–7 kb deletion was found in two affected sisters (Figure 7c). In M29, a deletion removing *PKD1* exons 1–15 and extending 5′ of the gene to include at least *E4F1* (a region of 120–175 kb) was defined. The deletion was confirmed in three affected family members by MLPA (Figure 7d) and other methods (see Table 1 and Figures 1 and 4 for details).

Screening of *PKD2* revealed an intragenic deletion of exon 5 in family M363 that was confirmed by LR-PCR (Table 1, Figure 5).

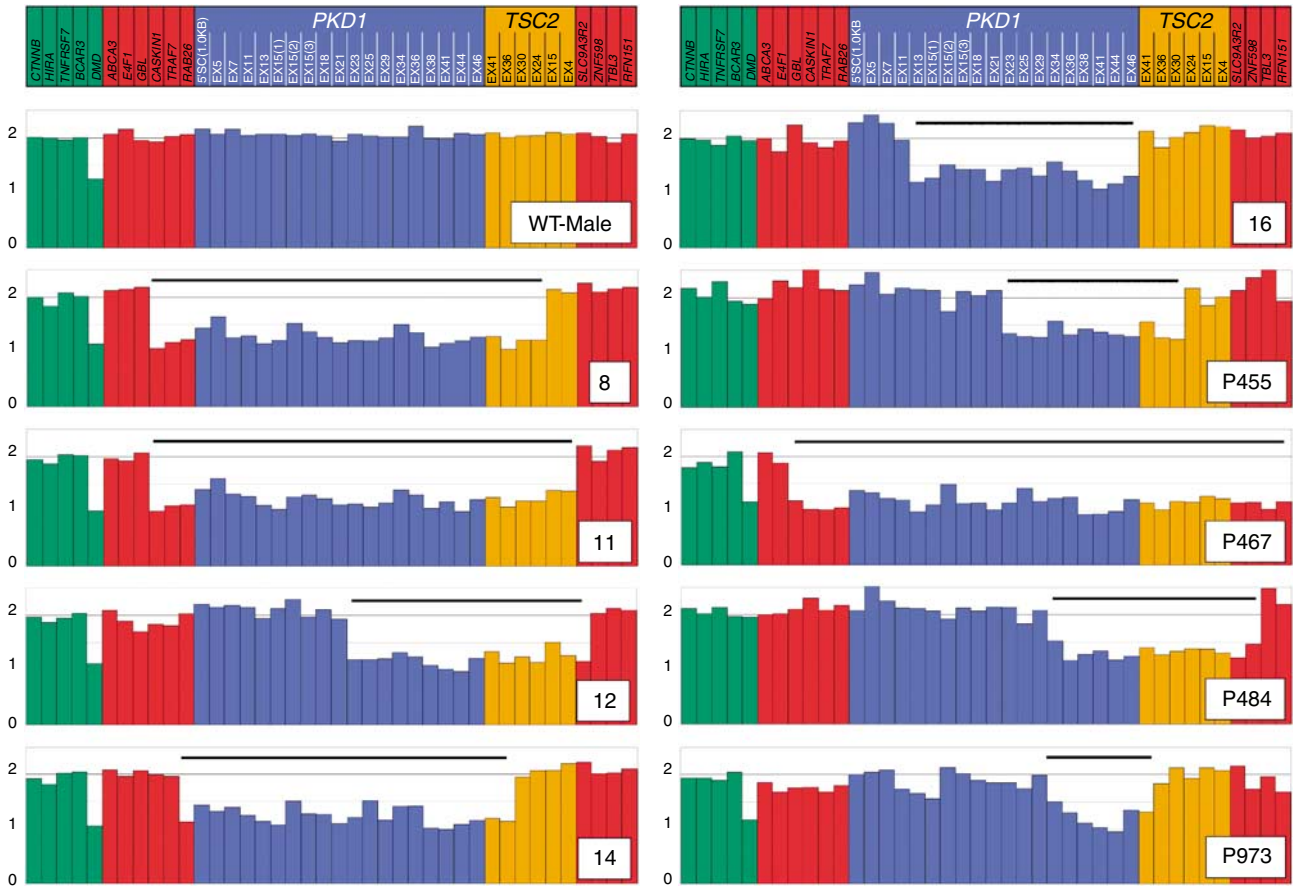

Figure 2 | Examples of MLPA results from *PKD1/TSC2*-CGS cases. MLPA data for *PKD1* (blue), *TSC2* (orange), flanking probes (red), and control markers (green) is indicated, with details of specific probes at the top. The *y* axis shows copy number at the diploid (2) and haploid (heterozygous deleted; 1) level. The pedigree identifier is indicated and the deleted region shown with a black bar. Cases 8, 11, 12, 14, and 16 have previously been described (Table 1).

Novel *PKD1/TSC2* contiguous gene deletions

MLPA analysis of patients with tuberous sclerosis and severe PKD revealed seven new CGS cases (see Figure 1 and Table 1 for details):

P467 had childhood seizures, mild mental retardation and an atrial rhabdomyoma. Cystic kidneys were not diagnosed until 31 years, but he had ESRD following a left nephrectomy at 33 years. Original gel-based screening did not detect a deletion but MLPA showed a large deletion of >240 kb, removing the entire *PKD1* and *TSC2* genes (Figure 2). In retrospect, the negative gel results were due to deletion of all tested probes.

P484 had facial angiofibromas, hypopigmented macules, and a hepatic angiomyolipoma with PKD detected by ultrasound at 12 years. At 30 years, she had a left nephrectomy because of serious bleeding, and a serum creatinine = 1.3 mg/100 ml. MLPA revealed a deletion of 100–120 kb (Figure 2).

P455 presented at 2 years with seizures and behavioral problems and had massively cystic kidneys and hypertension. MLPA revealed a deletion removing *PKD1* exons 23–46 and 3′ *TSC2* to exon 30 (Figure 2).

P973 was diagnosed with PKD and TSC at 5 years, and at 11 years the kidneys were significantly enlarged (13.5 and 14.5 cm), but with normal function. MLPA indicated a deletion removing *PKD1* exons 34–46 and at least *TSC2* exon 41 (Figure 2).

Novel mosaic CGS cases

P974 developed multiple cortical tubers, seizures, and enlarged kidneys at less than 1 year. Her present serum creatinine = 0.76 mg/100 ml at 14 years. MLPA showed a mosaic deletion of *PKD1* exons 25–46 and all of *TSC2*. Gel analysis confirmed a mosaic deletion of ~60 kb (Figure 6a and b).

M214 was diagnosed at 6 months with enlarged kidneys, which were decompressed. TSC was diagnosed at 13 years with facial angiofibromas and by 23 years renal angiomyolipoma developed that required embolization. Her present serum creatinine = 1.5 mg/100 ml at 43 years. MLPA detected a mosaic deletion of 40–55 kb (Figure 6a).

P444 had hyperechogenic, enlarged kidneys detected *in utero* and TSC diagnosed by the detection of cerebral hamartomas. At 12 years, she is hypertensive with enlarged

kidneys (17 and 15.5 cm) but normal function (serum creatinine = 0.68 mg/100 ml). MLPA detected an 8–14 kb mosaic deletion (Figure 6a).

DISCUSSION

We have developed an MLPA assay to rapidly screen for large rearrangements causing ADPKD and the *PKD1/TSC2*-CGS, improving diagnostics for these disorders. Samples can readily be assayed in a 96-well plate format with results available within 2 days, in contrast to labor intensive gel or fluorescence *in situ* hybridization analysis. The screen covers genomic regions around *PKD2* (120 kb) and *PKD1/TSC2* (320 kb), with a probe density of one per 1.4 kb in the compact *PKD1* gene (except IVS1), and one per exon in *PKD2*. This probe density is likely to detect the vast majority of large deletion mutations; smaller changes to *PKD1* are generally evident as altered LR-PCR products.[5] The utility of the assay was shown by detection and defining 25 previously detected deletions, plus characterizing six new *PKD1*, one *PKD2*, and seven *PKD1/TSC2* mutations. During the preparation of this paper a similar MLPA scheme for *PKD1* was described, but no intragenic deletions were detected.[23]

A single-mismatch between *PKD1* and the six *PKD1*-pseudogenes was sufficient for locus specificity when the mismatch was placed adjacent to the ligation site at the 3′ end of the short probe. This mismatch presumably destabilized annealing of the short probe so that ligation could not occur. The MLPA system employed here has distinct advantages over other described methods. In particular, the Luminex Flex-Map bead system allows a higher level of multiplexing than capillary electrophoresis systems; 88 different probes can be utilized in one assay.

In all tested cases where more than one adjacent MLPA probe had reduced signal, LR-PCR or gel methods identified a deletion. However, in three cases signal reduction for a single probe was associated with a rare base-pair change: *PKD1*:8681_8688del9 (2894delANS), exon 23; *PKD1*:11186A→C (H3729P), exon 39 and *TSC2*:4767G→A (P1589P), exon 36. The 8681del9 deletion was previously described as a rare polymorphic deletion removing a duplication that has occurred since *PKD1* and the *PKD1P1-P6* diverged.[5] This difference was used to generate the exon 23-specific probe (Supplementary Table S1). The substitutions 11186A→C and the 4767G→A lay at the −2 position of the *PKD1*:exon 39 short probe and the −1 position of the *TSC2*:exon 36 short probe, respectively. These cases illustrate that rare single nucleotide polymorphisms (SNPs) can disrupt ligation and amplification and, therefore, signal difference associated with just one MLPA probe needs to be tested by LR-PCR and sequencing.

In common with other CGS cases, all the newly described cases had TSC with significant renal cystic disease.[15,18] Although in our original report we stressed the infantile presentation in non-mosaic cases,[18] others have highlighted cases where PKD was only evident much later.[19] The four non-mosaic cases had moderately severe cystic disease

Table 1 | Details of deletions/duplications of study patients

		MPLA data[a]						Mosaicism[b]			
ID	ty[c]	cen flank	cen del	tel del	tel flank	Size (kb)[d]	conf[e]	Y/N	%	*P*	Ref[f]
A. PKD1/TSC2 – CGS											
2	del	PKD1:5′1.0	PKD1:EX5	TSC2:EX24	TSC2:EX15	57–68	PF; FH	N			14,18
3	del	GBL	CASKIN1	SLC9A3R2	ZNF598	150–165	PF; FH	N			14,18
4	del	PKD1:EX18	PKD1:EX21	TSC2:EX30	TSC2:EX24	29	PF; FH	Y	49	<0.01	14,18
6	del	E4F1	GBL	TSC2:EX24	TSC2:EX15	145–170	PF; FH	Y	72	<0.01	14,18
7	del	CASKIN1	TRAF7	TSC2:EX30	TSC2:EX24	95–107	PF; FH	N			18
M7	del	CASKIN1	TRAF7	TSC2:EX30	TSC2:EX24	95–107	PF; FH	Y	33	<0.01	18
8	del	GBL	CASKIN1	TSC2:EX24	TSC2:EX15	120–145	PF; FH	N			18
9	del	PKD1:EX29	PKD1:EX34	TSC2:EX30	TSC2:EX24	20–25	PF	N			18
11	del	GBL	CASKIN1	TSC2:EX4	SLC9A3R2	145–165	PF; FH	N			18
12	del	PKD1:EX21	PKD1:EX23	SLC9A3R2	ZNF598	~75	PF; FH	N			18
13	del	PKD1:EX29	PKD1:EX34	TSC2:EX36	TSC2:EX30	12–18	PF	N			18
F13	del	ND	ND	ND	ND	12–18	PF; GE	Y	~15[g]	NS	18
14	del	TRAF7	RAB26	TSC2:EX36	TSC2:EX30	76–89	PF; FH	N			18
15	del	PKD1:5′1.0	PKD1:EX5	TSC2:EX36	TSC2:EX30	41–46	PF; FH	N			18
16	del	PKD1:EX11	PKD1:EX13	PKD1:EX46	TSC2:EX41[h]	31	PF; LP	N			18
17	del	PKD1:EX46[h]	TSC2:EX41	TSC2:EX41	TSC2:EX36	1.1	PF, GE	N			18
19	del	E4F1	GBL	TSC2:EX4	SLC9A3R2	175–195	PF; FH	Y	53	<0.01	18
20	del	PKD1:EX7	PKD1:EX11	TSC2:EX36	TSC2:EX30	35–40	PF; FH	Y	26	<0.01	18
22	del	RAB26	PKD1:5′ 1.0	TSC2:EX15	TSC2:EX4	85–95	PF; FH	Y	47	<0.01	18
77-4	del	PKD1:EX15(2)	PKD1:EX15(3)	RNF151	ND	~2100	PF; FH	N			2
M214	del	PKD1:EX13	PKD1:EX15(1)	TSC2:EX24	TSC2:EX15	40–55	N	Y	28	<0.01	N
P444	del	PKD1:EX36	PKD1:EX38	TSC2:EX36	TSC2:EX30	8–14	N	Y	48	<0.01	N
P455	del	PKD1:EX21	PKD1:EX23	TSC2:EX30	TSC2:EX24	~30	PF	N			N
P467	del	E4F1	GBL	RFN151	ND	>240	N	N			N
P484	del	PKD1:EX29	PKD1:EX34	ZNF598	TBL3	100–120	N	N			N
P973	del	PKD1:EX29	PKD1:EX34	TSC2:EX41	TSC2:EX36	~15	PF	N			N
P974	del	PKD1:EX23	PKD1:EX25	TSC2:EX4	SLC9A3R2	~60	PF	Y	30	<0.01	N

Table 1 | Continued

		MPLA data[a]						Mosaicism[b]				
ID	ty[c]	cen flank	cen del	tel del	tel flank	Size (kb)[d]	conf[e]	Y/N	%	*P*	Designation	Ref[f]
B. PKD1												
P95	del	PKD1:EX34	PKD1:EX37	PKD1:EX46	TSC2:EX41	5.5	FG, NB, RP	N			IVS34_EX46 del5.5 kb	2
P98	del	PKD1:EX29	PKD1:EX34	PKD1:EX34	PKD1:EX36	2	FG, RP, NB	N			IVS30_IVS34 del2 kb	2
100001	del	PKD1:EX13	PKD1:EX15(1)	PKD1:EX15(1)	PKD1:EX15(2)	1.076	LS, S	N			3815_4890 del1076	5
120395	del	PKD1:EX7	PKD1:EX11	PKD1:EX15(2)	PKD1:EX15(3)	5.604	FG, LS	N			2200_5946 del5604;insAC	5
301157	del	PKD1:EX25	PKD1:EX29	PKD1:EX38	PKD1:EX39	9.214	FG, LS, S	N			IVS26-243_IVS38-13 del9214	5
F301157	del	ND	ND	ND	ND	9.214	LS	Y	15[g]	NS	IVS26-243_ IVS38-13del9214	N
393936	del	PKD1:EX23	PKD1:EX25	PKD1:EX29	PKD1:EX34	3.065	FG, LS, S	N			IVS24-28_IVS30+ 48del3065	5
M29	del	ABCA3	E4F1	PKD1:EX15(3)	PKD1:EX18	120–175	FG, S	N				N
M143	del	PKD1:EX15(3)	PKD1:EX18	PKD1:EX21	PKD1:EX23	1.2–7.5	S	N				N
100009	del	RAB26	PKD1:5′1.5	PKD1:5′1.0	PKD1:IVS2	~2.5	FG, S	N				N
259940	dup	PKD1:EX15(3)	PKD1:EX18	PKD1:EX18	PKD1:EX21	0.246	LS	N			IVS17+1_7328 dup246	N
407132	del	TRAF7	RAB26	PKD1:EX21	PKD1:EX23	48–87	N	N				N
493328	del	PKD1:EX11	PKD1:EX13	PKD1:EX34	PKD1:EX36	21	LS	N			IVS11+357_IVS34+ 1992del21 kb	N
C. PKD2												
P964	del	ND	ABCG2	SAPP1	ND	ND	FH; Cy	N				12
M363	del	PKD2:EX6	PKD2:EX5	PKD2:EX5	PKD2:EX4	5.722	LS	N			IVS4+452_IVS5-965 del5722	N

cen, centromeric; conf, confirmation; Cy, cytogenetics; del, deleted; dup, duplication; flank, flanking; FH: FISH, fluorescence *in situ* hybridization; GE, gel electrophoresis; LP: LR-PCR, long range PCR; LS, LR-PCR and sequencing; N, none; ND, not determined; N, no; PF: PFGE, pulsed field gel electrophoresis; S, segregation demonstration; tel, telomeric; ty, type; Y, yes; NS, not significant; NB, northern blotting; FG, field inversion gel electrophoresis; RP, RT-PCR.
[a]Closest MLPA probes flanking the gene and deleted on the centromeric and telomeric side: ND.
[b]Mosaicism: YN; % of cells with deleted allele; *P*-value, significance that MLPA detected deletion was different from full or no deletion: NS.
[c]Type of rearrangement: del/dup.
[d]Size of deletion: ND.
[e]Confirmation of the del/dup: PF; FH; conventional GE; LP; LS; N; S; Cy; FG; NB; RP.
[f]Reference (ref); Novel (N).
[g]Estimated from gel analysis.
[h]Exon disrupted but 3′ to MLPA probe.

(resulting in ESRD at 33 years in P467), but the diagnosis was not always made during infancy; at 2, 5, 12 or 31 years. Interestingly, in the three mosaic cases, PKD was always diagnosed before 1 year, showing the severity of cystic disease and penetrance of the mutation (at least in leukocyte DNA) does not always strongly correlate.

The MLPA assay will be useful in all TSC patients with significant renal cystic disease to differentiate CGS cases from those with TSC and PKD inherited as separate gene mutations.[24,25] Approximately 60% of TSC cases are *de novo*; 80% due to *TSC2* mutation,[26] and practically all described CGS cases are *de novo* or inherited from a mosaic case.[18] Previously, mosaicism has been found to be commonly associated with large *TSC* deletions,[15,18] a finding echoed here in the CGS. Mosaic cases were readily detected by the MLPA assay (except where the deleted allele was present in $<20\%$ cells) and represented three of seven new cases; 40% of all *PKD1/TSC2* deletion families had a mosaic case (Table 1 and Figure 1). Identifying mosaicism is important for determining risk in siblings of the patient.

This study determined that the level of large rearrangements causing typical ADPKD is ~4%, a little higher than estimates from gel-based studies,[9] and included the first duplication. These numbers somewhat underestimate total *PKD1* deletions as those that also disrupt *TSC2* have the CGS phenotype. One *PKD2* single exon deletion was found, indicating that these mutations are also relatively rare. Although the level of large *PKD1* or *PKD2* rearrangements is relatively low, 31% of sequence determined mutation negative cases had large deletions, indicating that MLPA would be a useful addition to any clinical, mutation-based test. It is worth noting that the four new large rearrangements found in CRISP were from the mutation negative group, not those with likely missense changes,[5] increasing the probability that the missense changes are truly pathogenic. This assay will also prove useful for screening for somatic loss of heterozygosity in cyst lining cells.[27]

All previously described large deletions in typical ADPKD were intragenic;[2,5,9] however, in this study two deletions extended centromeric to *PKD1*. One (407132) removed at

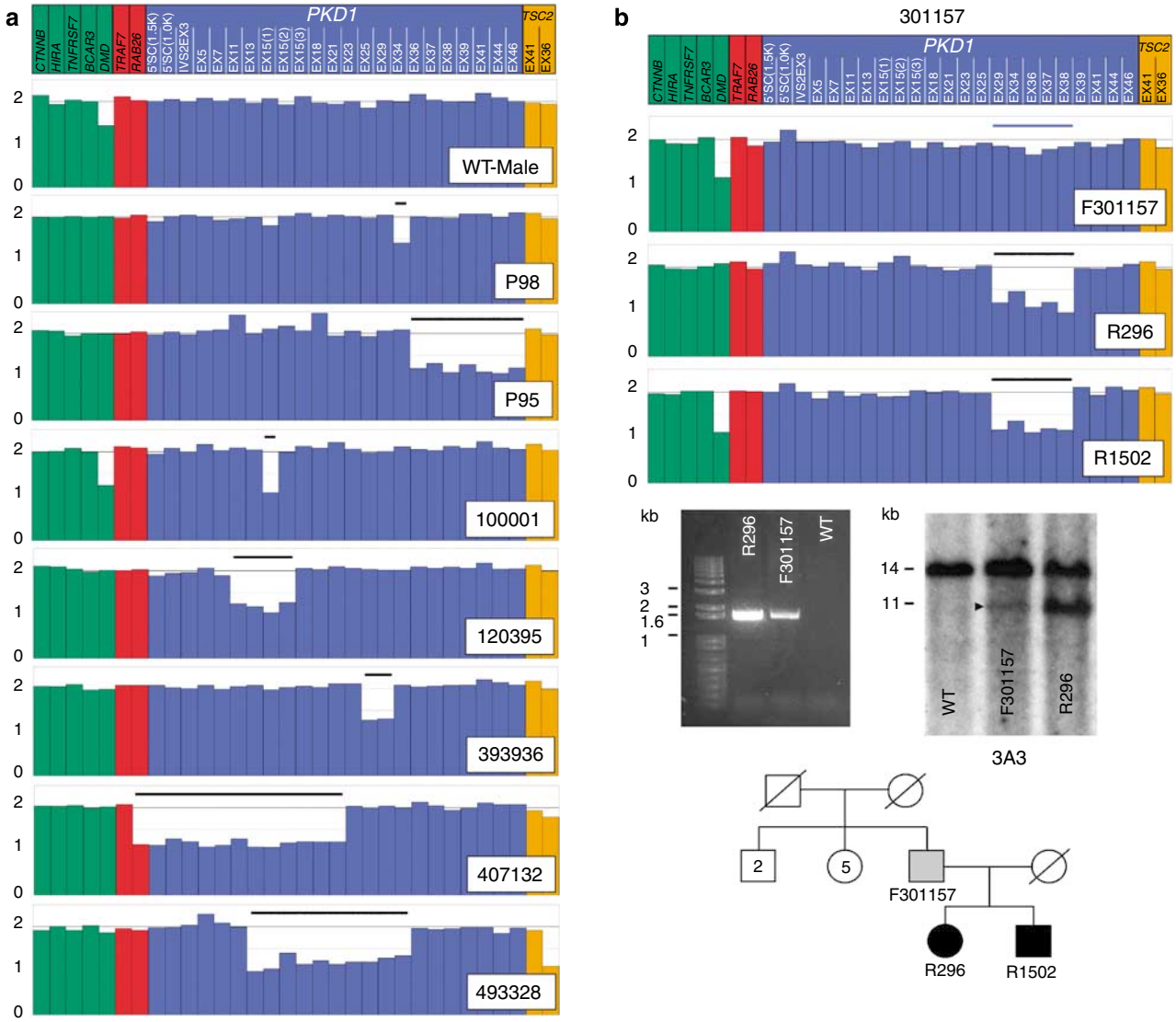

Figure 3 | Analysis 2 *PKD1* deletion mutations. (**a**) MLPA data showing *PKD1* deletion cases (colors and markings as indicated for Figure 2). Further probes within and immediately 5′ to *PKD1* were used to provide higher resolution analysis for these cases. P98, P95, 100001, 120395, and 393936 have been previously described (Table 1). (**b**) Family 301157 is a mosaic for a *PKD1* deletion. (Top): MLPA showing deletion in two siblings, R296 and R1502, but not visible in the affected father, F301157. (Middle, left): PCR with primers in *PKD1* exons 25 and 41 generated a 1.7 kb breakpoint fragment in R296, which is at a reduced level in F301157, and not in the wild type (WT). (Middle, right): Hybridization of a *Bam*H1 digest with *PKD1* cDNA probe 3A3 (exons 43–46). The wild-type fragment (14 kb) is reduced to 11 kb due to the deletion (R296; Figure 4). The deleted product is seen at a low level in the father (F301157; arrowhead), indicating mosaicism. (Bottom): Pedigree showing no known PKD in the grandparents and seven siblings (two brothers and five sisters), and mosaicism indicated by shading in the father.

least the closest flanking gene, *RAB26*. In the second (M29), the deletion extended 100–150 kb centromeric from *PKD1* and disrupted up to 10 genes (Figure 1). This is a family with a sibship of 15, 7 of whom are known to have ADPKD (Figure 7c); however, no unusual clinical features were noted. This is significant because the M29 deletion extends further centromeric than any in the *PKD1*/*TSC2*-CGS cases. Previously, a CGS case with a ~280 kb deletion, probably disrupting up to *ABCA3*, had craniofacial and limb abnormalities (acrofacial dysostosis), which is not characteristic of TSC.[28] This phenotype may be due to disruption of *ABCA3* or other genes (*RNPS1*, *DCI*, or *DNASE1L2*) deleted in the published case but not disrupted in M29. Recessive mutations to *ABCA3* are associated with severe neonatal surfactant deficiency,[29] but there is no reported heterozygous phenotype. None of the other implicated genes have been associated with a disease phenotype. Fine mapping of both mutations by modifying the MLPA assay may help to understand acrofacial dysostosis possibly associated with this region.

The renal disease severity of large *PKD1* deletion cases as a group (or families individually) was unremarkable. For instance, the average age at ESRD was 55.7 years, similar to the PKD1 average. Family 100009, with exon 1 deleted, had

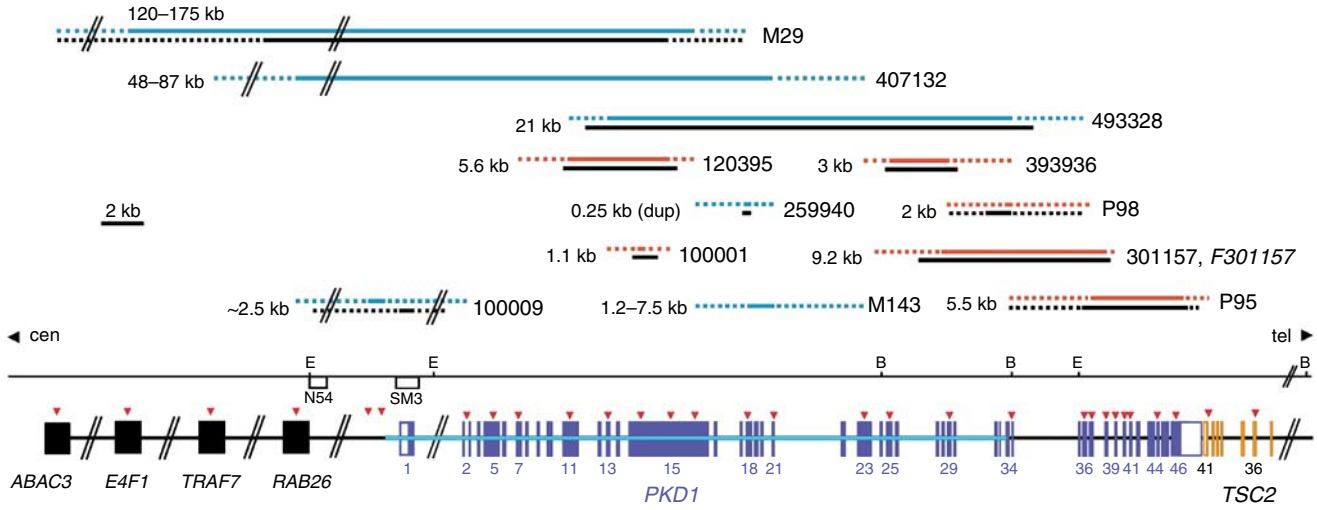

Figure 4 | Diagram showing the regions deleted or duplicated in the *PKD1* cases. Restriction sites for *Eco*RI (E) and *Bam*HI (B), plus hybridization probes (open boxes) and centromeric (cen) and telomeric (tel) directions are indicated. The intron/exon structure of *PKD1* (light blue bar indicates the duplicated area) and 3′ end of *TSC2* are shown at the bottom, plus *PKD1* flanking genes and positions of MLPA probes (red arrowheads). MLPA detected rearrangements are in red (or blue for novel changes) and black bars indicate disrupted regions determined by FIGE, PCR, and sequencing. Pedigree identifiers, plus deletion (duplication; dup) sizes, are indicated, with the mosaic case (F301157) italicized.

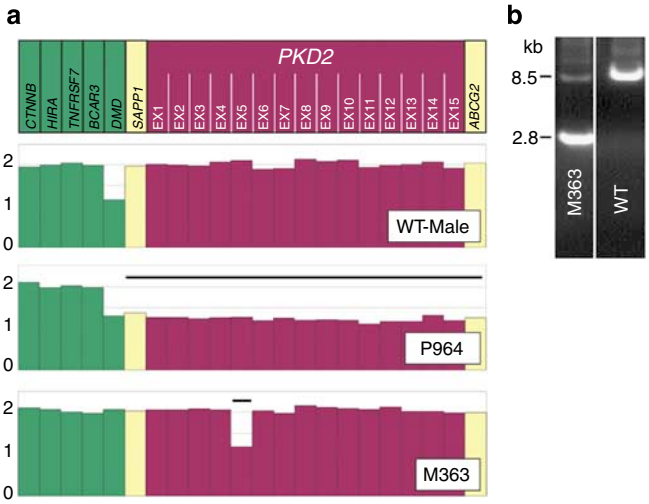

Figure 5 | Analysis of *PKD2* deletions. (**a**) MLPA analysis of patient with large deletion of *PKD2* region (P964[12]) and case with deletion of exon 5 (M363). (**b**) LR-PCR with primers in exons 4 and 6 showed a ~2.8 kb breakpoint fragment in M363 compared to 8.5 kb in the wild type (WT).

three cases with large renal volumes (>2,800 ml), in the top 5% of the age-corrected CRISP volumes.[30] However, two other family members had average (or even below average) volumes, probably indicating that genetic modifiers rather than allelic effects have the greatest influence on the severity of renal disease.[31]

Three of the twelve *PKD1* large rearrangement families were molecularly proven to have *de novo* mutations. One consequence of a significant level of *de novo* mutations, by analogy with TSC and the *PKD1/TSC2*-CGS, is that a significant level of mosaic cases may be expected. One such case was detected in F301157. Recently, the first case of mosaicism in ADPKD was described.[32] Diagnosing mosaicism is important as it may have prognostic implications; although F301157 developed ESRD at 55 years even though the deleted allele was rare in leukocyte DNA (but presumably more common in the kidney). Furthermore, mosaicism is important to consider when determining the risk of transmission to children and the probability that siblings will be affected. In particular, it can be a confounding factor when screening for a living renal donor in offspring from the mosaic case.[32]

MATERIALS AND METHODS

Sample collection and DNA isolation

The study was approved by relevant Institutional Review Boards and Ethics Committees, and participants gave informed consent. Clinical and family records were reviewed to collect a full clinical history.

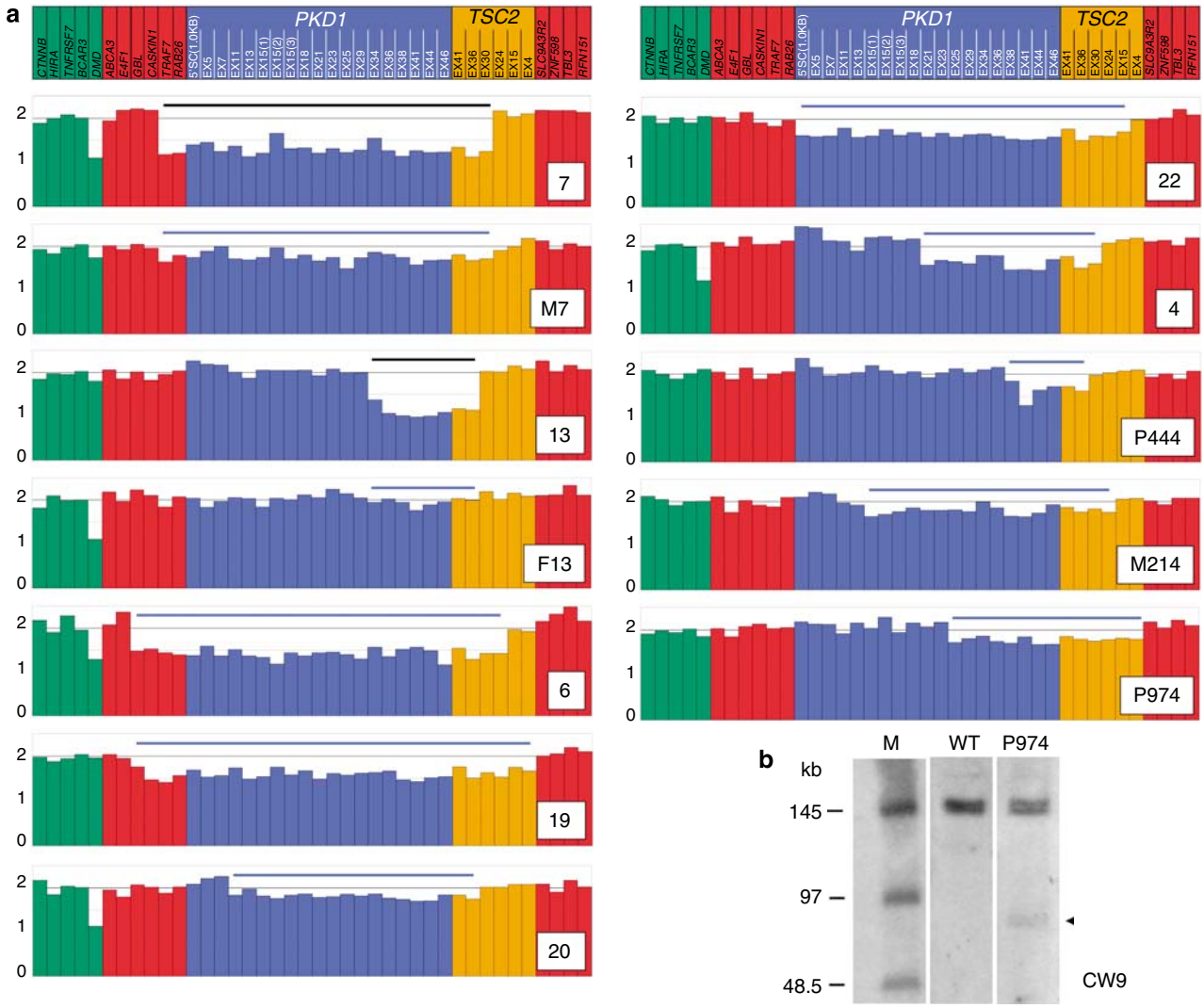

Figure 6 | Characterizations of mosaic deletions associated with the *PKD1/TSC2*-CGS. (**a**) MLPA analysis of mosaic *PKD1/TSC2*-CGS cases. Reduction in copy number appears less than 50% as all cells do not have the deletion (see Table 1 for estimate of level of mosaicism). Full deletion is indicated by a black bar and mosaic deletions with a blue bar. M7 and F13 are mosaic parental samples of cases with deletions (7 and 13, respectively). The M7 deletion is evident but the F13 deletion (previously estimated as present in 15% of alleles) is not seen by MLPA. Subjects 7, M7, 13, F13, 19, 20, and 22 have previously been described (Table 1). Cases 4 and 6 were described in the same publication, but not identified as mosaics. (**b**) PFGE of *Nru*I-digested P974 DNA hybridized with CW9 showing a deleted fragment, ~60 kb smaller than normal present at a low level (arrowhead), indicating mosaicism.

DNA was isolated from blood samples with the Puregene DNA Purification System (Gentra Systems; Minneapolis, MN, USA). Details of new and previously published cases are summarized in Table 1. Field inversion gel electrophoresis and pulsed field gel electrophoresis employed liquid and agarose block DNA, respectively, as previously described.[2,6,18] Details of probes and microsatellites employed, as illustrated in Figure 1, and a comprehensive restriction map of the area, have previously been described.[2,6,18,33] Methods for LR-PCR have been described[8] and primer sequences are available on request.

MLPA probe design

Two adjacent gene-specific oligo probes were designed within regions of target genes without known SNPs (Supplementary Table S1).[34,35] The short probe had 24–30 bp of complementary sequence 5′ appended with a universal forward primer (5′-acattttgct gccggtca-3′); and the long probe had 40–50 bp of complementary sequence 5′-phosphorylated and 3′ appended with complementary Luminex (Luminex Corporation; Austin, TX, USA) FlexMAP bead sequence and a universal reverse primer (5′-gtcctttgtcgatactgg-3′). All probes were synthesized by Integrated DNA Technologies (Coralville, IA, USA); short and long probe scale/purification was 100 nmol/HPLC and 250 nmol/PAGE, respectively.

Due to the presence of six *PKD1-pseudogenes* (*PKD1P1-P6*), *PKD1* versus *PKD1P1-P6* mismatches were identified to design *PKD1* exons 1–33-specific probes. MacVector (MacVector Inc.; Cary, NC, USA) was used to establish ClustalW sequence alignments. Localization of a single base-pair mismatch at the ligation site (the extreme 3′ end) of the short probe, and clustering of any other available mismatches to the remainder of the short probe, resulted in *PKD1*-specific MLPA probes (Supplementary Table S1 for probe details and positions of mismatches).

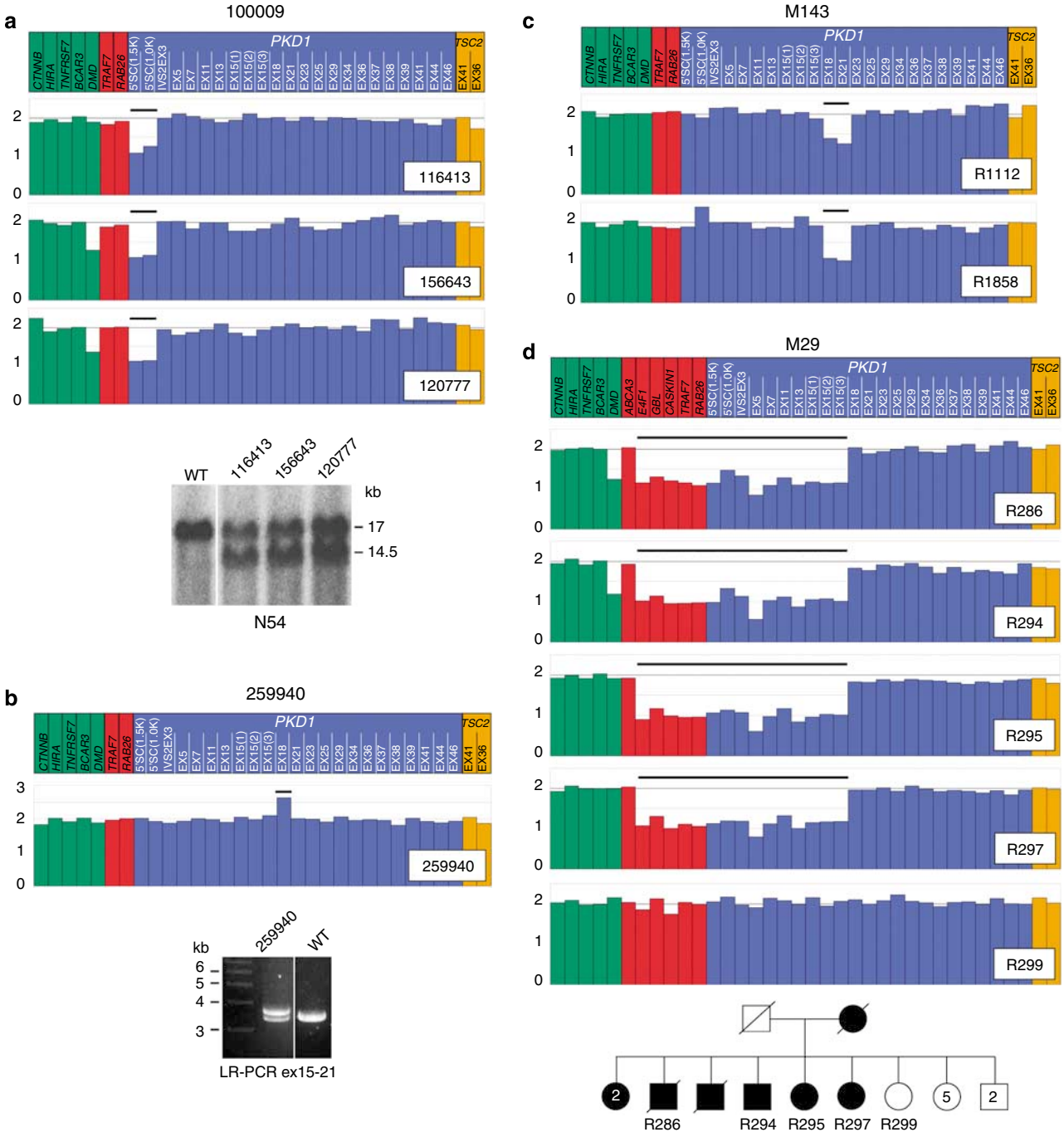

Figure 7 | Pedigree analysis of *PKD1* rearrangement cases. (**a**) Family (100009) with deletion of *PKD1* exon 1. (Top): MLPA analysis showing deletion of two probes located 5′ to exon 1 in three affected family members. (Bottom): *Eco*R1-digested genomic DNA hybridized with N54 shows a ~2.5 kb smaller deletion fragment in these cases. (**b**) Family 259940 has a duplication: (top) MLPA shows increased signal with the exon 18 probe and (bottom) LR-PCR from exons 15–21 reveals a ~250 bp larger product in the patient. (**c**) MLPA in M143 showing deletion of exons 18–21 in two affected siblings. (**d**) Family M29 with large *PKD1* deletion. (Top): MLPA of four siblings showed a deletion of 120–175 kb extending centromeric to *PKD1* and including *E4F1* but not *ABCA3*. Bottom: partial pedigree of this large family indicating a total of 15 siblings, 7 affected.

MLPA probe hybridization, ligation, and PCR reactions

For hybridization, a mix containing 2.5 fmol/μl of each probe was prepared in 1 × Tris-EDTA (TE; Fisher Scientific; Fair Lawn, NJ, USA). Genomic DNA (400 ng) was denatured at 95 °C for 5 min, cooled to 25 °C and a solution of 1.5 μl MLPA probe mix and 1.5 μl of Ligase-65 MLPA Buffer (MRC Holland; Amsterdam, the Netherlands) added and hybridized at 60 °C for 16–24 h.

The ligation reaction mix contained: 25 μl of water; 3 μl of Ligase-65 Buffer A; 3 μl of Ligase-65 Buffer B; and 1 μl of Ligase-65 (MRC Holland). The ligation solution (32 μl) was added to the DNA

reaction tube, incubated at 54 °C for 15 min., followed by a 95 °C enzyme denaturation, 5 min, and 4 °C cooling, 5 min.

PCR amplification of the ligated probes employed the mix: 27.5 μl water; 1.5 μl of 50 mM $MgCl_2$; 4 μl dNTPs (2.5 mM each; Invitrogen Corporation, Carlsbad, CA, USA); 0.25 μl each F-/R-universal primer (20 μM; Integrated DNA Technologies); and 1 μl Platinum Taq Polymerase (Invitrogen). The MLPA ligation product (10 μl) was added to 40 μl of the PCR mix and amplification employed the following program: 95 °C, 5 min: 23 cycles of 95 °C, 30 s; 60 °C, 30 s; 72 °C, 30 s; 72 °C, 20 min; and 4 °C, 5 min.

Luminex FlexMAP bead hybridization and analysis

The Luminex FlexMAP technology employs flow cytometry and color-coded microspheres to rapidly identify up to 88 different samples (in this case MLPA probes) in one assay. A Luminex FlexMAP bead mix corresponding to the MLPA probes to be analyzed was prepared by mixing the FlexMAP beads (Luminex; part no. L100-Uxxx-01, xxx = bead no.: 001–099; 2000 beads per DNA sample) with 40 μl per DNA sample of 1 × tetramethylammonium chloride (Sigma-Aldrich; St Louis, MO, USA).

The PCR reaction mixture (10 μl) was added to 40 μl of the FlexMAP bead mix and hybridized at 37 °C for 1 h. A 250 μl tetramethylammonium chloride solution containing 2 μl of Streptavidin, R-Phycoerythrin (Invitrogen) was prepared; 25 μl of this solution was aliquoted, along with 50 μl of the FlexMAP bead hybridization mixture, to a flow cytometer 96-well analysis plate (Luminex). The samples were hybridized at 37 °C for 1 h in the dark and analyzed using a Luminex-100 flow cytometer.

The resulting data were deconvoluted according to relative copy number versus both the external control genes as well as a wild-type normal control female sample using the GeneMarker software (Softgenetics, LLC; State College, PA, USA). The 'normal' signal copy number threshold was set at 2.0 ± 0.4. An X-linked control gene (versus wild-type normal control male sample), as well as multiple gene-specific (*PKD1*, *PKD2*, and *PKD1*/*TSC2*) characterized deletion samples, was utilized as internal controls to confirm the specificity of the MLPA probes. MLPA probe gene copy numbers were exported to Excel (Microsoft Corporation; Redmond, WA, USA) and reported as copy number vs gene probe histograms.

Assessing mosaicism

The means and standard deviations (s.d.) of probe variability were determined for the normal and deleted regions and limits set at 3 × s.d. of the moving average using the method of quality control charts.[36] Deletions with a mean value for the deleted region falling outside of these 3 × s.d. limits ($P = 0.01$) were considered to be mosaics and the percentage of cells with the deleted allele is shown in Table 1.

DISCLOSURE

All the authors declared no competing financial interests.

ACKNOWLEDGMENTS

The patients, their families, and clinicians, including Dr A Britland, Keighley, UK, are thanked for taking part in the study. Members of CRISP who collected radiological and clinical information: WM Bennett, CM Meyers, LK Moen, JP Miller, JE Bost, BF King, LH Wetzel, DA Baumgarten, PJ Kenney, J Mahan, B Stafford, L Stevens, K Cornwell, D Watkins, S Langley and P Trull are also thanked. The study was supported by NIDDK grant DK58816 and CRISP support from NIDDK Cooperative Agreements: DK56943, DK56956, DK56957, and DK56961. WC Wong was supported as a Mayo Clinic Summer Undergraduate Research Fellow (SURF).

SUPPLEMENTARY MATERIAL

Table S1. Details of *PKD1*, *TSC2*, *PKD2,* Flanking and Control MLPA Probe Sequences.

Supplementary material is linked to the online version of the paper at http://www.nature.com/ki

REFERENCES

1. Torres VE, Harris PC, Pirson Y. Autosomal dominant polycystic kidney disease. *Lancet* 2007; **369**: 1287–1301.
2. European Polycystic Kidney Disease Consortium. The polycystic kidney disease 1 gene encodes a 14 kb transcript and lies within a duplicated region on chromosome 16. *Cell* 1994; **77**: 881–894.
3. Hughes J, Ward CJ, Peral B *et al.* The polycystic kidney disease 1 (*PKD1*) gene encodes a novel protein with multiple cell recognition domains. *Nat Genet* 1995; **10**: 151–160.
4. Mochizuki T, Wu G, Hayashi T *et al.* PKD2, a gene for polycystic kidney disease that encodes an integral membrane protein. *Science* 1996; **272**: 1339–1342.
5. Rossetti S, Consugar MB, Chapman AB *et al.* Comprehensive molecular diagnostics in autosomal dominant polycystic kidney disease. *J Am Soc Nephrol* 2007; **18**: 2143–2160.
6. European Chromosome 16 Tuberous Sclerosis Consortium. Identification and characterization of the tuberous sclerosis gene on chromosome 16. *Cell* 1993; **75**: 1305–1315.
7. Loftus BJ, Kim U-J, Sneddon VP *et al.* Genome duplications and other features in 12 Mbp of DNA sequence from human chromosome 16p and 16q. *Genomics* 1999; **60**: 295–308.
8. Rossetti S, Chauveau D, Walker D *et al.* A complete mutation screen of the ADPKD genes by DHPLC. *Kidney Int* 2002; **61**: 1588–1599.
9. Ariyurek Y, Leeuwen IL, Spruit L *et al.* Large deletions in the polycystic kidney disease 1 (*PKD1*) gene. *Hum Mutat* 2004; **23**: 99.
10. HGMD: Human Gene Mutation Database In: http://www.hgmd.cf.ac.uk, 2008.
11. Torra R, Badenas C, San Millan JL *et al.* A loss-of-function model for cystogenesis in human autosomal dominant polycystic kidney disease type 2. *Am J Hum Genet* 1999; **65**: 345–352.
12. Velinov M, Kupferman J, Gu H *et al.* Polycystic kidneys and del (4)(q21.1q21.3): further delineation of a distinct phenotype. *Eur J Med Genet* 2005; **48**: 51–55.
13. Boehm D, Bacher J, Neumann HP. Gross genomic rearrangement involving the TSC2-PKD1 contiguous deletion syndrome: characterization of the deletion event by quantitative polymerase chain reaction deletion assay. *Am J Kidney Dis* 2007; **49**: e11–e21.
14. Brook-Carter PT, Peral B, Ward CJ *et al.* Deletion of the *TSC2* and *PKD1* genes associated with severe infantile polycystic kidney disease—a contiguous gene syndrome. *Nat Genet* 1994; **8**: 328–332.
15. Kozlowski P, Roberts P, Dabora S *et al.* Identification of 54 large deletions/duplications in TSC1 and TSC2 using MLPA, and genotype-phenotype correlations. *Hum Genet* 2007; **121**: 389–400.
16. Laass MW, Spiegel M, Jauch A *et al.* Tuberous sclerosis and polycystic kidney disease in a 3-month-old infant. *Pediatr Nephrol* 2004; **19**: 602–608.
17. Longa L, Scolari F, Brusco A *et al.* A large *TSC2* and *PKD1* gene deletion is associated with renal and extra-renal signs of the autosomal dominant polycystic kidney disease. *Nephrol Dial Transpl* 1997; **12**: 1900–1907.
18. Sampson JR, Maheshwar MM, Aspinwall R *et al.* Renal cystic disease in tuberous sclerosis: role of the polycystic kidney disease 1 gene. *Am J Hum Genet* 1997; **61**: 843–851.
19. Smulders YM, Eussen BH, Verhoef S *et al.* Large deletion causing the TSC2-PKD1 contiguous gene syndrome without infantile polycystic disease. *J Med Genet* 2003; **40**: E17.
20. Torra R, Badenas C, Aspinwall R *et al.* A 40-kilobases deletion involving the *PKD1* and *TSC2* genes causes a contiguous gene syndrome: tuberous sclerosis and polycystic kidneys. *Am J Kidney Dis* 1998; **31**: 1038–1043.
21. Hogervorst FB, Nederlof PM, Gille JJ *et al.* Large genomic deletions and duplications in the BRCA1 gene identified by a novel quantitative method. *Cancer Res* 2003; **63**: 1449–1453.
22. Schouten JP, McElgunn CJ, Waaijer R *et al.* Relative quantification of 40 nucleic acid sequences by multiplex ligation-dependent probe amplification. *Nucleic Acids Res* 2002; **30**: e57.
23. Kozlowski P, Bissler J, Pei Y *et al.* Analysis of PKD1 for genomic deletion by multiplex ligation-dependent probe assay: absence of hot spots. *Genomics* 2008; **91**: 203–208.

24. Griffin MD, Gamble V, Milliner DS *et al.* Neonatal presentation of autosomal dominant polycystic kidney disease with a maternal history of tuberous sclerosis. *Nephrol Dial Transpl* 1997; **12**: 2284–2288.
25. Woerner AC, Au KS, Williams AT *et al.* Tuberous sclerosis complex and polycystic kidney disease together: an exception to the contiguous gene syndrome. *Genet Med* 2006; **8**: 197–198.
26. Sancak O, Nellist M, Goedbloed M *et al.* Mutational analysis of the TSC1 and TSC2 genes in a diagnostic setting: genotype—phenotype correlations and comparison of diagnostic DNA techniques in tuberous sclerosis complex. *Eur J Hum Genet* 2005; **13**: 731–741.
27. Watnick TJ, Torres VE, Gandolph MA *et al.* Somatic mutation in individual liver cysts supports a two-hit model of cystogenesis in autosomal dominant polycystic kidney disease. *Mol Cell* 1998; **2**: 247–251.
28. Dauwerse JG, Bouman K, van Essen AJ *et al.* Acrofacial dysostosis in a patient with the TSC2-PKD1 contiguous gene syndrome. *J Med Genet* 2002; **39**: 136–141.
29. Shulenin S, Nogee LM, Annilo T *et al.* ABCA3 gene mutations in newborns with fatal surfactant deficiency. *N Engl J Med* 2004; **350**: 1296–1303.
30. Grantham JJ, Torres VE, Chapman AB *et al.* Volume progression in polycystic kidney disease. *N Engl J Med* 2006; **354**: 2122–2130.
31. Paterson AD, Magistroni R, He N *et al.* Progressive loss of renal function is an age-dependent heritable trait in type 1 autosomal dominant polycystic kidney disease. *J Am Soc Nephrol* 2005; **16**: 755–762.
32. Connor A, Lunt PW, Dolling C *et al.* Mosaicism in autosomal dominant polycystic kidney disease revealed by genetic testing to enable living related renal transplantation. *Am J Transplant* 2008; **8**: 232–237.
33. Peral B, Gamble V, Strong C *et al.* Identification of mutations in the duplicated region of the polycystic kidney disease 1 (*PKD1*) gene by a novel approach. *Am J Hum Genet* 1997; **60**: 1399–1410.
34. NCBI: Single Nucleotide Polymorphism In: National Library of Medicine and National Institutes of Health (NIH) (ed). *National Center for Biotechnology Information (NCBI) dbSNP database*. http://www.ncbi.nlm.nih.gov/SNP/, 2008.
35. ADPKD: Mutation Database (PKDB) In: http://pkdb.mayo.edu, 2008.
36. Duncan AJ. *Quality Control and Industrial Statistics*. Richard D. Irwing Inc.: Homewood, 1976.